



Liquid Coating with Variable Thermal Conductivity on a Pipe under Influence of Thermal Radiation and Heat Generation

Lim Yeou Jiann^{1,*}, Sharidan Shafie¹, Zuhaila Ismail¹, Noraihan Afiqah Rawi¹, Ahmad Qushairi Mohamad¹

¹ Department of Mathematical Sciences, Faculty of Science, Universiti Teknologi Malaysia, 81310 Johor Bahru, Johor, Malaysia

ARTICLE INFO

Article history:

Received 27 July 2022

Received in revised form 5 September 2022

Accepted 7 September 2022

Available online 10 November 2022

Keywords:

Carreau Fluid; thermal radiation; variable thermal conductivity; heat generation

ABSTRACT

Flow over a pipe or an elongated cylinder is widely applied in many engineering processes like wire coating and pipe coating. This encourages the present study to examine the fluid flow and heat transfer over a horizontal stretching cylinder with the impact of temperature-reliant thermal conductivity and thermal radiation. The influence of heat generation is also considered. The Carreau rheology model is applied to represent the liquid coating. The similarity technique is used to simplify the developed governing equations and then solved by the homotopy analysis method. The effects of the pertinent parameters such as the thermal conductivity parameter and Weissenberg number on the fluid field and heat transfer are studied by applying the calculated series of analytical solutions, which are scrutinized through graphs and tables. The Nusselt number has a negative function with the radiation and thermal conductivity parameters. Furthermore, the Weissenberg number affects the velocity and temperature profiles differently in conditions $n < 1$ and $n \geq 1$, respectively. The present results are essential in optimizing the pipe coating process.

1. Introduction

Carreau fluid has recently been concerned by plenty of researchers due to its importance in the coating process, polymeric suspensions, food processing, wire coating, and chemical engineering. The Carreau model incorporates the Newtonian model and the power-law model. It was proposed by Carreau [1] to overcome the inadequate power-law constitutive relation while predicting the viscosity with an extremely huge or extremely small shear rate. El Misery *et al.*, [2] deliberated the separation flow of a Carreau fluid that is incompressible in a uniform tube through peristaltic motion. A similar problem was considered by Akbar *et al.*, [3] by including the impact of mass and thermal transfer. Akbar *et al.*, [4] scrutinized the boundary layer stagnation-point flow of Carreau liquid over a shrinking sheet in the presence of a magnetic field. Two different sets of numerical solutions were obtained, and the effect of the shrinking parameter, magnetic number, and Weissenberg number, on the fluid flow was analyzed. Further, Hayat *et al.*, [5] elucidated the impact of the Newton

* Corresponding author.

E-mail address: jiann@utm.my

<https://doi.org/10.37934/cfdl.14.11.102118>

boundary conditions on a Carreau fluid flow past through a stretched sheet. The authors observed that the velocity and temperature profiles have an opposite behavior under the effect of the power-law index.

Khan [6] emphasized the consequence of nonlinear stretching surface on the Carreau boundary layer fluid flow and heat transmission. Hayat *et al.*, [7] discussed the properties of Soret and Brownian motion on the nanofluid with Carreau rheology toward a heated elongating plane. The three-dimensional Carreau fluid flow and heat transmission through a bidirectional elongating sheet were scrutinized by Khan *et al.*, [8]. The consequence of irregular thermal radiation was also considered. The authors found that the shear-thickening fluid and shear-thinning fluid provide a conflicting behavior on the velocity distribution for the various value of the Weissenberg number.

Many industrial or manufacturing procedures involve flow over a stretching cylinder such as paper construction, pipe coating, polymer, crude oil refinement, glass fiber production, photographic films, and drawing wire. Generally, the flow over a cylinder is assumed to be axisymmetric, resulting in the governing equations containing a transverse curvature term. This term has a significant influence on the velocity field. In view of this, Wang [9] theoretically discussed a viscous, incompressible, and steady fluid flows over a stretching tube. This pioneering work has inspired some researchers to investigate the Carreau fluid flow which has been induced by a stretching or shrinking tube. Salahuddin [10] elucidated the flow of Carreau fluid toward a stretching cylinder. The impact of the various embedding parameters such as the power-law index, Weissenberg value, and curvature parameter on the fluid movement was discussed. However, in the study, only the shear-thickening fluid is focused on.

Moreover, the heat transfer in Carreau fluids over a stretched cylinder has relevant applications in sciences and engineering. Thus, Khan *et al.*, [11] have studied the impact of the melting heat phenomenon, and the stretching rate on the Carreau liquid flows over a cylinder. The finding shows that the boundary layer thickness of the momentum is getting larger. Salahuddin *et al.*, [12] constructed a study on Carreau nanofluid near a linear enlarging cylinder with the effect of slip flow, chemical reaction, and magnetic field. The authors concluded that the fluid flows have a higher velocity, concentration, and temperature than the fluid through a stretching sheet. Hayat *et al.*, [13] studied the consequence of Newtonian heating and thermal radiation on a Carreau fluid movement induced by a stretching plane with a chemical reaction. The authors detected that the temperature distribution is enhanced for larger radiation parameters and smaller Weissenberg numbers. Khan *et al.*, [14] highlighted the significance of the magnetic field and Ohmic heating on the thermal and mass transmission of nano-Carreau fluid through a sloping heated elongating cylinder.

The impact of the curvature parameter, power-law index, and Weissenberg number on the rate of heat transfer was discussed. Gangadhar *et al.*, [15] presented the effect of temperature jump, and slip boundary conditions on the MHD Carreau Cattaneo-Christov heat fluid over a stretching cylinder. The reflection of the velocity and temperature profile for the various value of the Biot number was graphically displayed and analyzed. Gopal and Kishan [16] numerically elaborated the unsteady flow of Carreau fluid past a shrinking cylinder. The impact of the unsteadiness, thermal relaxation parameter, and Weissenberg number on the distribution of fluid motion and heat was analyzed. Recently, Song *et al.*, [17] analyzed the impact of the melting heat phenomenon and bioconvection on a nano-Carreau fluid flow driven by a nonuniform stretching cylinder. Akram *et al.*, [18] acknowledged the significance of the abnormal heat generation on Carreau fluid that contains nanoparticles. Besides, the authors have also considered the same configuration as concerned by Song *et al.*, [17]. The effect of the nonlinear stretching and shrinking rate of a cylinder on an MHD non-Newtonian fluid was discussed by Kardri *et al.*, [19]. The influence of the heat source and viscous

dissipation have been considered, the author found that the shear stress and heat transmission are enhanced by the curvature of the cylinder.

So far, all the aforementioned literature has treated the thermal conductivity of the ambient fluid to be constant. However, in real-world circumstances, such properties demand variable characteristics. The thermal conductivity of liquid metals is approximated to be directly proportional to the temperature from 0 °F to 400 °F [20-25]. Recently, Khan *et al.*, [26] investigated the effect of combined electrical and MHD fields on the flowing of nano-Carreau fluid passing a stretching oscillatory porous surface in the existence of temperature-dependent thermal conductivity. The authors observed that a high conduction process is produced when the parameter for thermal dependence conductivity is increased. Furthermore, Abbas *et al.*, [27] acknowledged the characteristic of the MHD Carreau fluid with variable thermal conductivity under the influence of variable viscosity toward a permeable sheet that is stretched. The heat transport with convective heat flux was discussed. The characteristics of the velocity, concentration, and heat fields under the impact of diverse fluid parameters such as the suction parameter, Weissenberg number, Lewis number, and magnetic parameter were analyzed graphically. Recently, the effect of the modification in thermal conductivity on a bioconvection non-Newtonian fluid movement was studied by Yin *et al.*, [28]. The flow was assumed across a stretching tube, and the results revealed that the variable thermal conductivity parameter increases the rate of heat exchange. Furthermore, Nabwey *et al.*, [29] investigated the bioconvection of the nanofluid with Carreau rheology behavior. The impact of the sloping stretchable cylinder and the variable conductivity in thermal on the fluid properties was discussed. More relevant investigations about the significance of the inconstant thermal conductivity that is dependent on the temperature can be found in Hayat *et al.*, [30], Jain *et al.*, [31], Salahuddin *et al.*, [32], Malik *et al.*, [33], Rangi *et al.*, [34], Ewis [35].

To the best of the author’s knowledge, the research on the impact of stretching rate, heat generation, and thermal radiation on the fluid field and heat transmission of a Carreau fluid passing a cylinder under the influence of temperature-reliant thermal conductivity has not been conducted in the literature yet. Hence, the objective of the current investigation is to explore the behavior of the heat transport and Carreau fluid flow through a stretching cylinder in attendance of temperature-dependent conductivity, heat source, and thermal radiation. Due to the effectiveness of the HAM in solving highly non-linear differential equations, HAM is applied in the current study. The developed Mathematica solver by Liao [36-38], which is named BVP4c, is utilized to compute the solutions.

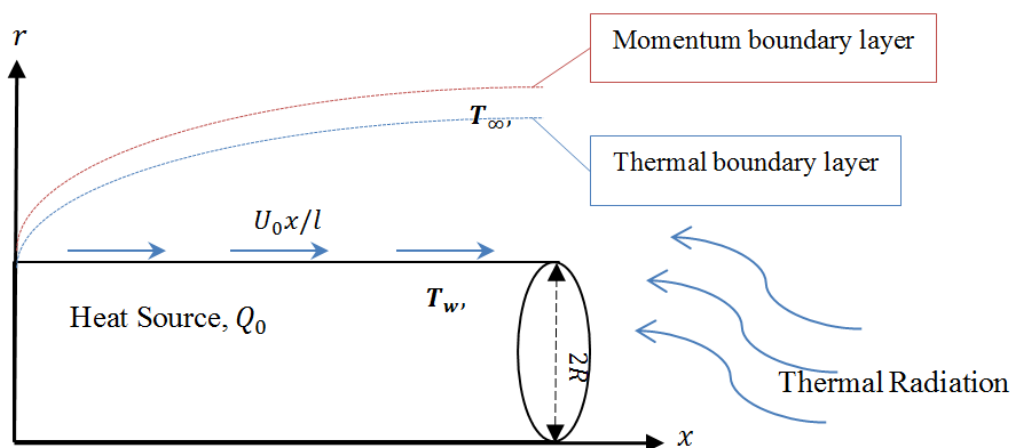


Fig. 1. Schematic diagram of fluid flow over a stretching pipe under the effect of heat source and thermal radiation

2. Methodology

2.1 Mathematical Formulation

An incompressible axisymmetric flow of steady two-dimensional Carreau fluid toward an elongating cylinder is studied in the present research. The r -axis is determined along the radial direction and the x -axis is measured along the axial direction, as presented in Figure 1. A cylinder with radius R and l characteristic length is considered. U_0 is the reference velocity, and the cylinder is stretched with a velocity U_0x/l . T_w is the temperature at the surface of the cylinder and T_∞ is assumed to be the ambient temperature. Carreau fluid model is applied to model the rheology of the fluid flow. The Cauchy stress tensor for Carreau fluid is written as [3, 5, 10, 12]

$$\tau_{ij} = \mu \mathbf{R}, \quad (1)$$

With

$$\frac{\mu - \mu_\infty}{\mu_0 - \mu_\infty} = \left[1 + (\Gamma \chi)^2 \right]^{\frac{n-1}{2}}. \quad (2)$$

Where the first kind Rivlin-Erickson tensor \mathbf{R} , the infinite-shear-rate viscosity μ_∞ , the viscosity of the shear rate μ , the power-law index n , the viscosity of the zero-shear rate μ_0 , and the material time constant Γ . χ is the shear rate and is expressed as

$$\chi = \sqrt{\frac{1}{2} \Delta} = \sqrt{\frac{1}{2} \sum_i \sum_j \chi_{ij} \chi_{ij}} = \sqrt{\frac{1}{2} \text{tr}(\mathbf{R}^2)}, \quad (3)$$

where the second invariant strain tensor is denoted by Δ . The current study deliberates the case for $\eta_\infty = 0$ and $\Gamma \chi < 1$, in the constitutive Equation (1) thus by binomial expansion, Equation (2) become

$$\mu = \mu_0 \left[1 + \frac{n-1}{2} (\Gamma \chi)^2 \right]. \quad (4)$$

Substitute Equation (4) into (1), and the stress tensor can be exhibited as

$$\tau_{ij} = \mu_0 \left[1 + \frac{n-1}{2} (\Gamma \chi)^2 \right] \mathbf{R}, \quad (5)$$

The governing equations of the fluid with the Carreau model are developed by utilizing the boundary layer approximation and are represented as

$$\frac{\partial(ru)}{\partial x} + \frac{\partial(rv)}{\partial x} = 0, \quad (6)$$

$$u \frac{\partial u}{\partial x} + v \frac{\partial u}{\partial r} = \nu \left(\frac{\partial^2 u}{\partial r^2} + \frac{1}{r} \frac{\partial u}{\partial r} + \frac{3\Gamma^2(n-1)}{2} \left(\frac{\partial u}{\partial r} \right)^2 \frac{\partial^2 u}{\partial r^2} + \frac{\Gamma^2(n-1)}{2r} \left(\frac{\partial u}{\partial r} \right)^3 \right), \quad (7)$$

where the kinematic viscosity is denoted by ν . The considered boundary conditions are

$$\begin{aligned} u &= \frac{U_0 x}{l}, \quad v = 0, \quad \text{at} \quad r = R, \\ u &\rightarrow 0, \quad \text{as} \quad r \rightarrow \infty. \end{aligned} \tag{8}$$

The energy equation of the Carreau fluid in the presence of temperature generation and thermal radiation on the stretching tube is given by

$$u \frac{\partial T}{\partial x} + v \frac{\partial T}{\partial r} = \frac{1}{r} \frac{\partial}{\partial r} \left(\alpha r \frac{\partial T}{\partial r} \right) - \frac{1}{\rho c_p} \frac{\partial q_r}{\partial r} + \frac{Q_0 (T - T_\infty)}{\rho c_p}, \tag{9}$$

with the density ρ , the thermal conductivity α , the thermal radiation q_r , the specific heat c_p , and the heat source Q_0 . Equation (9) is subjected to boundary conditions as

$$\begin{aligned} T &= T_w, \quad \text{at} \quad r = R, \\ T &\rightarrow T_\infty, \quad \text{as} \quad r \rightarrow \infty. \end{aligned} \tag{10}$$

The Rosseland approximation is applied to approximate the derivative of the thermal radiation. Following [28, 31, 39, 40], we have

$$\frac{\partial q_r}{\partial r} = \frac{-16\sigma^* T_\infty^3}{3k^*} \frac{\partial^2 T}{\partial r^2}. \tag{11}$$

Where σ^* defines the Stefan-Boltzmann constant and the mean absorption coefficient is denoted by k^* . Substitutes Equation (11) into Equation (9), thus obtaining

$$u \frac{\partial T}{\partial x} + v \frac{\partial T}{\partial r} = \frac{1}{r} \frac{\partial}{\partial r} \left(\alpha r \frac{\partial T}{\partial r} \right) - \frac{1}{\rho c_p} \frac{-16\sigma^* T_\infty^3}{3k^*} \frac{\partial^2 T}{\partial r^2} + \frac{Q_0 (T - T_\infty)}{\rho c_p}. \tag{12}$$

In the range between -17.78°C to 204.444°C , the thermal conductivity is linearly proportional to the temperature and can be assumed as $\alpha = \alpha_\infty (1 + \varepsilon\theta)$ [30, 32, 34]. α_∞ is the constant thermal conductivity at $\eta \rightarrow \infty$ and ε is the small quantity.

2.2. Similarly Transformation

Equations (12) and (6)-(7) are transformed into ordinary differential equations by utilizing the subsequent similarity variables[10, 32]

$$\eta = \sqrt{\frac{U_0}{\nu l}} \left(\frac{r^2 - R^2}{2R} \right), \quad \theta = \frac{T - T_w}{T_w - T_\infty}, \quad \psi = \sqrt{\frac{\nu U_0}{l}} x R f(\eta). \tag{13}$$

Substitute Equations (13) into Equations (6), (7), and (12). Equation (6) is automatically satisfied, and Equations (7) and (12) reduce to

$$\frac{3(n-1)}{2}We^2(1+2\lambda\eta)(\lambda f''' + (1+2\lambda\eta)f''^2 f''') + 2\lambda f'' + (1+2\lambda\eta)f''' + \frac{(n-1)}{2}We^2\lambda(1+2\lambda\eta)(f'')^3 + ff'' - (f')^2 = 0, \quad (14)$$

$$(1+2\lambda\eta)(1+\varepsilon\theta + \frac{4}{3}Rd)\theta'' + \left(2\lambda + Pr f + 2\lambda\varepsilon\theta + \frac{4}{3}\lambda Rd\right)\theta' + (1+2\lambda\eta)(\theta')^2 \varepsilon + Pr Q\theta = 0, \quad (15)$$

with boundary conditions

$$f(\eta) = 0, \quad \theta(\eta) = 1, \quad f'(\eta) = 1, \quad \text{at } \eta = 0, \quad (16)$$

$$f'(\eta) \rightarrow 0, \quad \theta(\eta) \rightarrow 0, \quad \text{as } \eta \rightarrow \infty.$$

where the prime indicates differentiation with respect to η , the curvature parameter λ , We is the Weissenberg number, the heat generation parameter Q , the Prandtl number is defined by Pr , and the radiation number Rd . These parameters are defined by

$$\lambda = \frac{1}{R}\sqrt{\frac{\nu l}{U_0}}, \quad We = \Gamma x \sqrt{\frac{U_0^3}{\nu l^3}}, \quad Q = \frac{lQ_0}{\rho c_p U_0}, \quad (17)$$

$$Pr = \frac{\nu}{\alpha_\infty}, \quad Rd = \frac{4\sigma^* T_\infty^3}{3k^* \alpha_\infty \rho c_p}.$$

Re_x is the Reynold number. The skin friction coefficient ($\frac{1}{2}C_f Re_x^{1/2}$) and the Nusselt number ($Nu Re_x^{-1/2}$) are represented as

$$\frac{C_f Re_x^{1/2}}{2} = f''(0) + \frac{n-1}{2}We^2 [f''(0)]^3, \quad (18)$$

$$\frac{Nu}{Re_x^{1/2}} = -\theta'(0). \quad (19)$$

Where $\sqrt{Re_x} = \sqrt{\frac{x^2 U_0}{\nu l}}$.

2.3. Homotopy Analysis Method

The homotopy technique for determining the solutions of the fluid movement and heat exchange of the Carreau fluid toward an elongating horizontal cylinder is demonstrated. Heat generation and thermal radiation are included in the energy equation. Besides, the impact of the variable thermal

conductivity has also been taken into consideration. The guessed and selected initial estimates and the linear operator are

$$f_0(\eta) = -(e^{-\eta} - 1), \quad \theta_0(\eta) = e^{-\eta}, \tag{20}$$

$$L_f = f''' + f'', \quad L_\theta = \theta'' + \theta'. \tag{21}$$

The above auxiliary linear operator has the following properties:

$$L_f(a_1 + a_2\eta + a_3e^{-\eta}) = 0, \quad L_\theta(a_4 + a_5e^{-\eta}) = 0. \tag{22}$$

Where $a_1, a_2, a_3, a_4,$ and a_5 are arbitrary constants. The k th deformation equations for Equations (14) and (15) are

$$L_f\{f_k(\eta) - \chi_k f_{k-1}(\eta)\} - \hbar_f R_{k-1}(N_f\{f(\eta : q)\}) = 0. \tag{23}$$

$$L_\theta\{\theta_k(\eta) - \chi_k \theta_{k-1}(\eta)\} - \hbar_\theta R_{k-1}(N_\theta\{f(\eta : q), \theta(\eta : q)\}) = 0. \tag{24}$$

$\hbar_\theta (\neq 0)$ and $\hbar_f (\neq 0)$ are the control convergence parameter for the energy and momentum equation, respectively. N_f and N_θ are nonlinear operators. q is the embedding parameter, and

$$\chi_k = \begin{cases} 0, & k \leq 1, \\ 1, & k > 1, \end{cases} \quad R_{k-1} = \frac{1}{(k-1)!} \frac{\partial^{k-1}}{\partial q^{k-1}} \Big|_{q=0},$$

with,

$$\begin{aligned} R_{k-1}(N_f\{f(\eta : q)\}) = & \left[\frac{3(n-1)}{2} We^2(1+2\lambda\eta) + \frac{(n-1)}{2} We^2(1+2\lambda\eta) \right] \left[\sum_{l=0}^{k-1} f_{k-1-l}'' \sum_{j=0}^l f_{l-j}'' f_l'' \right] + \\ & (1+2\lambda\eta)^2 \frac{3(n-1)}{2} We^2 \left[\sum_{l=0}^{k-1} f_{k-1-l}'' \sum_{j=0}^l f_{l-j}'' f_l''' \right] + \end{aligned} \tag{25}$$

$$\begin{aligned} & 2\lambda f_{k-1}'' + (1+2\lambda\eta) f_{k-1}''' + \left[\sum_{l=0}^{k-1} f_{k-1-l} f_l'' \right] - \left[\sum_{l=0}^{k-1} f_{k-1-l}' f_l' \right]. \\ R_{k-1}(N_\theta\{f(\eta : q), \theta(\eta : q)\}) = & (1+2\lambda\eta) \left(1 + \frac{1}{3} Rd \right) \theta_{k-1}'' + 2 \left(1 + \frac{2}{3} Rd \right) \lambda \theta_{k-1}' + \\ & QPr \theta_{k-1} + (1+2\lambda\eta) \varepsilon \left[\sum_{l=0}^{k-1} \theta_{k-1-l}' \theta_l' \right] + \tag{26} \\ & (1+2\lambda\eta) \varepsilon \left[\sum_{l=0}^{k-1} \theta_l' \theta_{k-1-l} \right] + 2\lambda \varepsilon \left[\sum_{l=0}^{k-1} \theta_{k-1-l} \theta_l' \right] + Pr \left[\sum_{l=0}^{k-1} f_{k-1-l} \theta_l' \right]. \end{aligned}$$

The established BVP4.0 (a Mathematica package) by [38] has been employed to calculate θ_k and f_k for $k \geq 1$ and then the solutions of the governing equations. The convergence control parameters \hbar_f and \hbar_θ are introduced to assure the convergence of the series solutions. The average residual error technique calculates the optimal k th-order approximation convergence control parameters. The residual error for \hbar_f and \hbar_θ are defined as

$$E_k^f(\hbar_f) = \frac{1}{Z+1} \sum_{i=0}^Z \left[N_f \left(\sum_{j=0}^k f_j(\eta_i) \right) \right]^2, \quad E_k^\theta(\hbar_\theta) = \frac{1}{Z+1} \sum_{i=0}^Z \left[N_\theta \left(\sum_{j=0}^k \theta_j(\eta_i) \right) \right]^2. \quad (27)$$

$$E_k^{Total}(\hbar_f, \hbar_\theta) = E_k^f(\hbar_f) + E_k^\theta(\hbar_\theta). \quad (28)$$

Where the step size $\delta\eta$, Z is an integer and $\eta_i = i(\delta\eta)$. For further information, the explanation and application of the HAM in different fields can be referred to in the book by [38]. the optimal values at the k th-order approximation of the convergence control (\hbar_f and \hbar_θ) are calculated by the minimum of the total error $E_k^{Total}(\hbar_f, \hbar_\theta)$.

3. Results and Discussions

The optimal convergence control parameters of momentum and energy equation for $\lambda = We = 0.1$, $Pr = 0.7$, $\varepsilon = Q = 0.2$, $Rd = 1$, and $n = 1.2$, from 1st order up to the 6th- order of estimation is showed in Table 1 respectively. Table 1 demonstrates that the total error reduces to 7.77228×10^{-3} from 3.62064×10^{-2} as increasing the order of approximations. The 6th-order optimal approximations convergence-control parameters are $\hbar_f = -1.48981$ and $\hbar_\theta = -0.557282$.

Table 1 shows the series of analytical solutions converging in $-1.48981 \leq \hbar_f \leq -0.809868$ for velocity profile and $-0.557282 \leq \hbar_\theta \leq -0.323611$ for temperature profile. For generality, the 3rd order of approximation of $\hbar_f = -1.29224$ and $\hbar_\theta = -0.47300$ (see Table 1) is chosen to calculate the results for the following analysis. In this way, the profile and total error residual against the order of calculation of the series solution for $\lambda = We = 0.1$, $\varepsilon = Q = 0.2$, $Pr = 0.7$, $Rd = 1$, and $n = 1.2$, are exhibited in Figure 2 and Table 2 respectively. The total residual error is indeed diminishing as the order of calculation increases (see Table 2 and Figure 2).

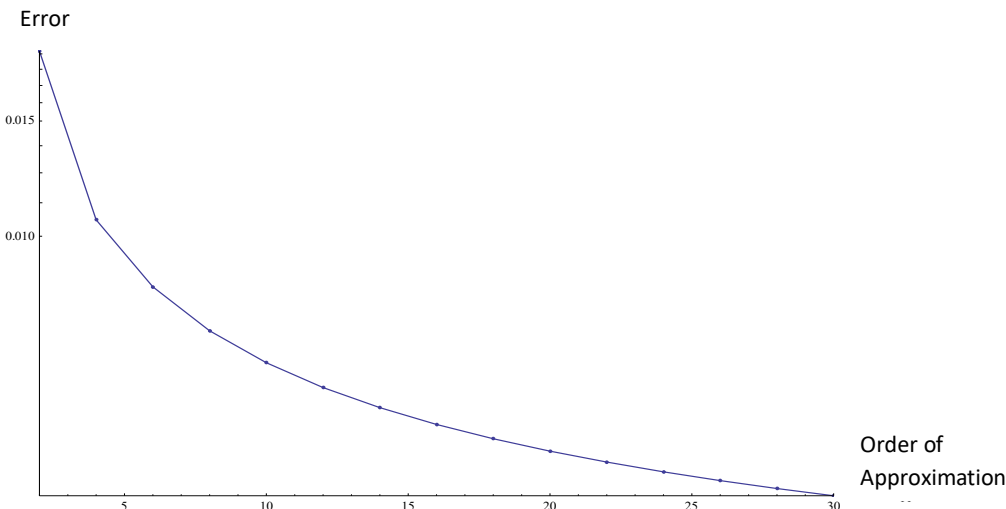


Fig. 2. The total error profile with $\hbar_f = -1.27994$ and $\hbar_\theta = -0.481381$ for $\lambda = We = 0.1$, $\varepsilon = Q = 0.2$, $Rd = 1$, $Pr = 0.7$, and $n = 1.2$.

Table 3 displays that the current results are in outstanding agreement with the former numerical results. For different values of λ in limiting cases, Table 3 compares the obtained solutions in a published journal paper with the present computed skin friction coefficient to validate the determined series solution. Furthermore, Table 4 presents that the present solutions for the local Nusselt number are well in agreement with the output given in [41] and [42]. The comparison for the local Nusselt number $-\theta'(0)$ is made for various magnitudes of Pr at $n = 1$ and $We = \lambda = Rd = \varepsilon = Q = 0$. This has enhanced our confidence in the solutions determined in the present study.

Table 1

k^{th} - orders of optimal approximation value of \bar{h}_f and \bar{h}_θ for $\lambda = We = 0.1, \varepsilon = Q = 0.2, Rd = 1, Pr = 0.7$, and $n = 1.2$

k	E_k^{Total}	\bar{h}_f	\bar{h}_θ
1	3.62064×10^{-2}	-0.809868	-0.323611
3	1.31479×10^{-2}	-1.29224	-0.47300
6	7.77228×10^{-3}	-1.48981	-0.557282

Table 2

The results of the square residual errors of the k^{th} -orders series solutions for $Pr = 0.7, \lambda = We = 0.1, \varepsilon = Q = 0.2, Rd = 1$, and $n = 1.2$

k	E_k^f	E_k^θ	E_k^{Total}	time-consuming (s)
10	8.39599×10^{-6}	6.39686×10^{-3}	6.40526×10^{-3}	104.845
20	4.40212×10^{-6}	4.68824×10^{-3}	4.69264×10^{-3}	2154.28
30	3.00318×10^{-6}	4.00734×10^{-3}	4.01034×10^{-3}	14720.7

Table 3

The results of the $C_f \sqrt{Re_x}$ in [11], [15], [43], and the present result for a range of values of curvature number λ with $n = 1$ and $We = 0$

λ	[11]	[43]	[15]	Present
0.1	-1.03698	-1.03698	-1.03698	-1.03989
0.3	-1.11117	-1.11114	-1.11115	-1.11881
0.7	-1.25705	-1.25701	-1.25702	-1.27297
1.0	-1.45337	-1.36387	-1.36387	-1.38641

Table 4

The results of the $Nu/\sqrt{Re_x}$ in [41], [42] and the present result for a range of values of Pr with $n = 1$ and $\lambda = Q = We = Rd = \varepsilon = 0$

Pr	[41]	[42]	Present
1	0.5832	0.5830	0.5835
10	2.3080	2.3080	2.3095

Figure 3 depicts an increment in the velocity when a higher number of λ , the curvature parameter, is applied. This is because the cylinder radius is negatively proportional to the curvature parameter λ . A bigger curvature number λ gives a smaller diameter of the cylinder, consequently reducing the touching region of the fluid with the cylinder surface. Hence, the resistive force generated by the surface of the tube reduces the fluid velocity.

Additionally, the curvature λ has caused the decline of the temperature at the exterior of the tube, as described in Figure 4, since less conduction of heat from the tube to the ambient fluid is allowed due to the narrow contact surface. While the λ increases the temperature distribution in the region far away from the pipe (cylinder).

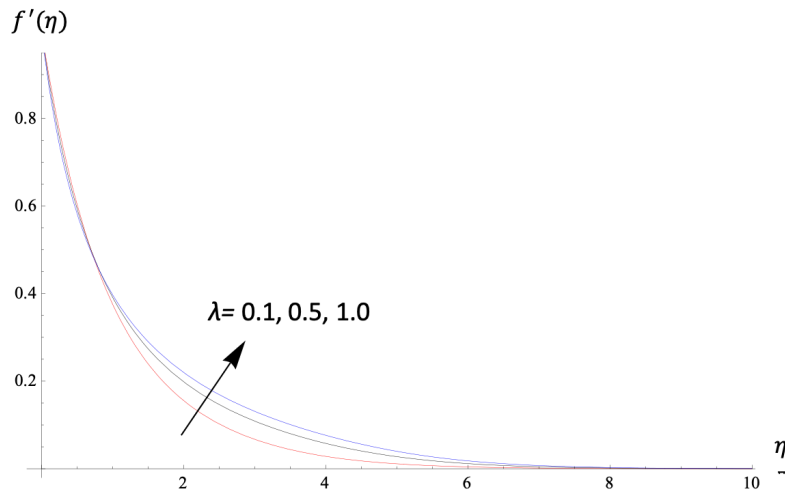


Fig. 3. $f'(\eta)$ against η for numerous magnitudes of λ with $n = 1.2$ and $We = 0.1$

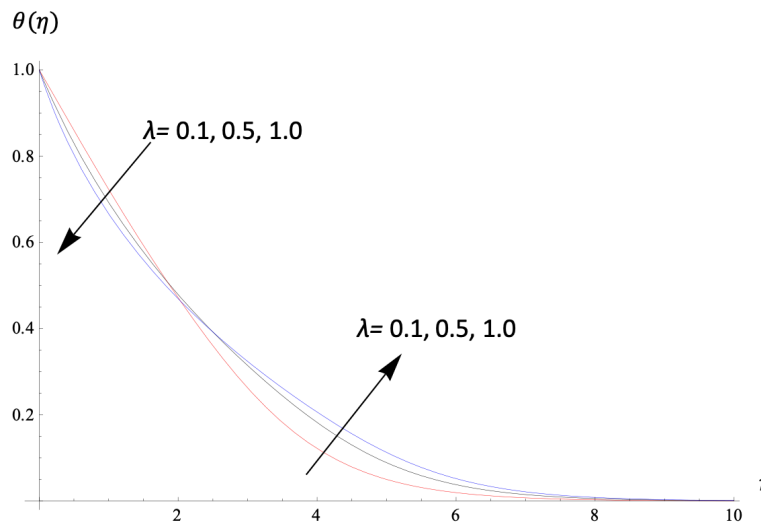


Fig. 4. $\theta(\eta)$ against η for various magnitudes of λ with $n = 1.2$, $We = 0.1$, $Pr = 0.7$, $Rd = 1$, and $\epsilon = Q = 0.2$

The space in the fluid is uplifted as the power-law index n has been improved. As a result, the velocity of the liquid is raised as seen in Figure 5. The larger n has made the momentum boundary layer becomes thicker. As n approaches 1, the fluid will behave Newtonian characteristics, leading to a decline in velocity as bigger viscosity is produced. The temperature distribution is diminished regarding the high value of the n , as illustrated in Figure 6.

Figure 8 demonstrates that the velocity profile of $n > 1$ (shear-thickening fluid), is positively proportional to the Weissenberg number We . Contradictory, there is a decrease in the velocity distribution for $n < 1$ (shear – thinning fluid), as illustrated in Figure 7. Physically, We is linearly dependent on Γ (the fluid relaxation time) as given in Equation (17). Accordingly, we assume $\Gamma\dot{\gamma} < 1$, thus the shear rate decreases, which results in $n < 1$ fluid with high viscosity but $n > 1$ fluid with low viscosity. In contrast, the shear-thinning fluid temperature increase for a larger number of the We (see Figure 9). However, a conflicting tendency is illustrated in Figure 10 for the shear-thickening fluid.

Figure 11 interprets that increment enhances the heat transfer in radiation parameters. An alike phenomenon is detected in Figure 12. The heat source parameter Q improves the thermal boundary layer. An improvement in temperature distribution is also achieved by increasing the ϵ parameter as

established in Figure 13. The thermal conductivity parameter ε increases the α of the fluid. Thus, more thermal is transported from the pipe (tube) to the Carreau fluid and thus induces an increment in kinetic energy of the fluid in particles which enhances the variation of thermal behavior.

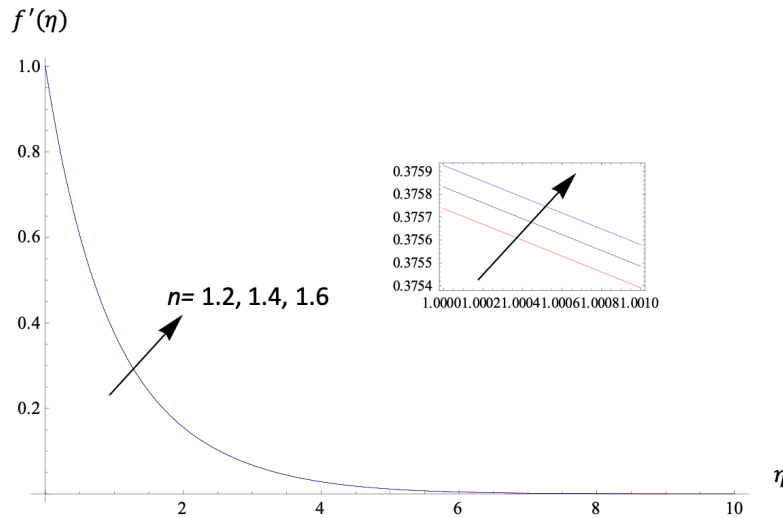


Fig. 5. $f'(\eta)$ against η for numerous magnitudes of n with $We = \lambda = 0.1$

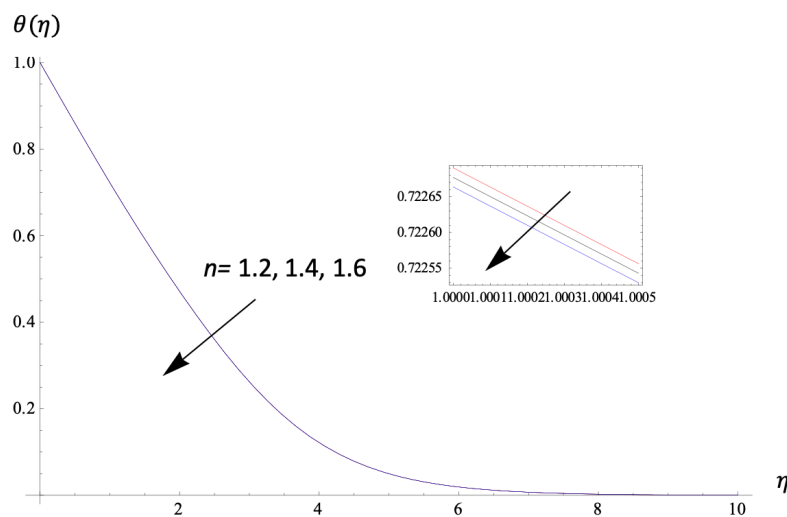


Fig. 6. $\theta(\eta)$ against η for various magnitudes of n with $\lambda = We = 0.1$, $Rd = 1$, $Pr = 0.7$, and $\varepsilon = Q = 0.2$

The behavior of local skin friction and local Nusselt number for a range of pertinent parameters Pr , λ , ε , n , We , Q , and Rd are directed in Tables 5 and 6, respectively. When $n = 1.2$, the We number increases the local skin friction. An opposite trend is noticed when $n = 0.5$ is applied. The curvature and power-law index, respectively, has enhanced the skin friction coefficient, as indicated in Table 5. Furthermore, the local Nusselt number $|\theta'(0)|$ is increased by the value of λ , Pr , We , and n , but a decrease happens when $n = 0.5$ for increasing the number of We . A decline is observed in the local Nusselt number $|\theta'(0)|$ when ε , Rd , and Q is enhanced respectively.

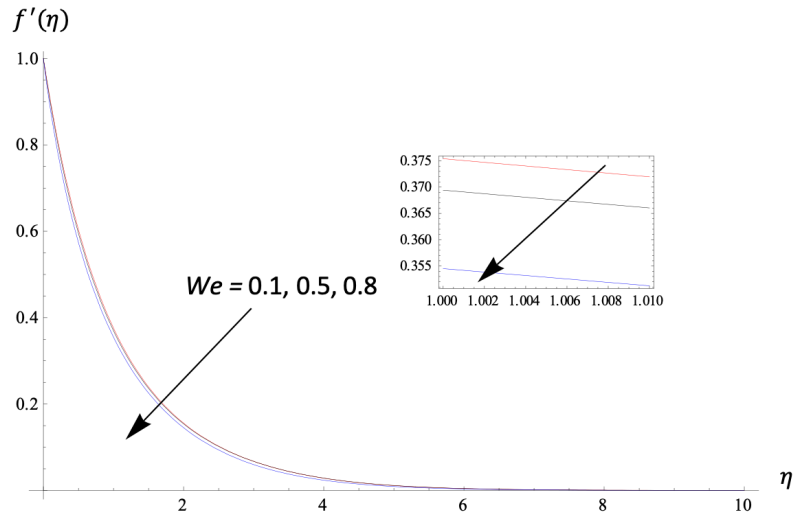


Fig. 7. $f'(\eta)$ against η for various magnitudes of We with $n = 0.5$ and $\lambda = 0.1$

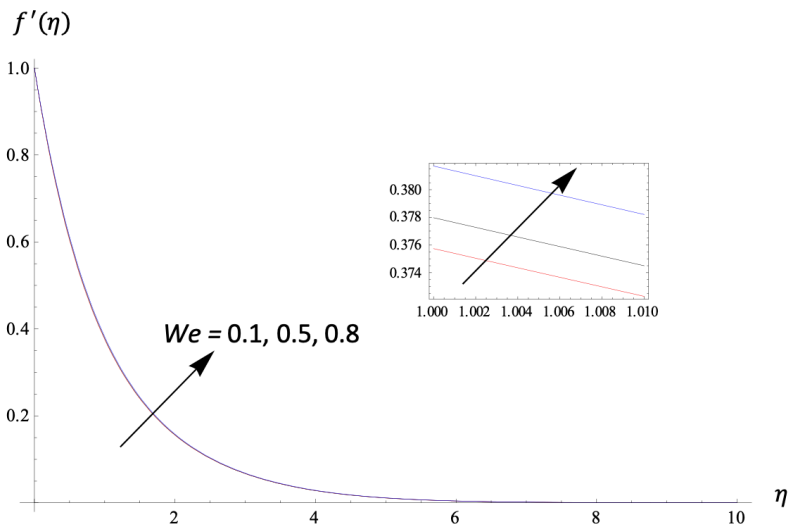


Fig. 8. $f'(\eta)$ against η for several values of We with $n = 1.2$ and $\lambda = 0.1$

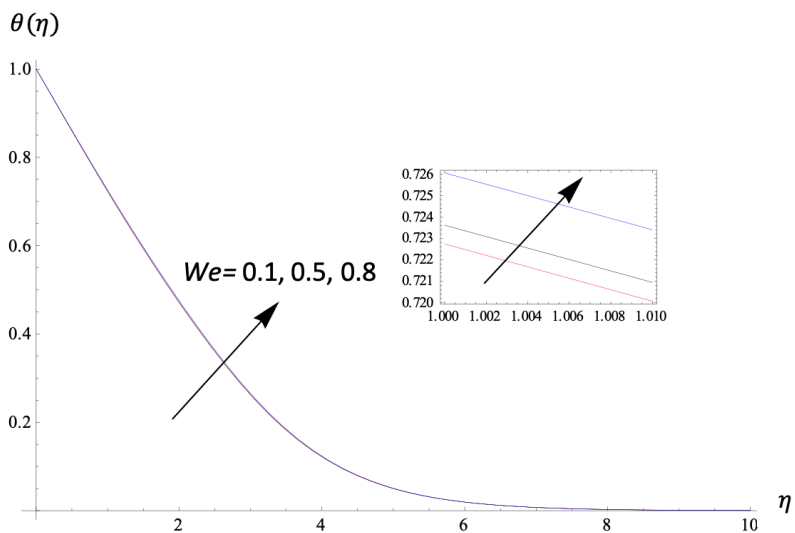


Fig. 9. $\theta(\eta)$ against η for various magnitudes of We with $n = 0.5$, $Pr = 0.7$, $Rd = 1$, $\lambda = 0.1$, and $\epsilon = Q = 0.2$

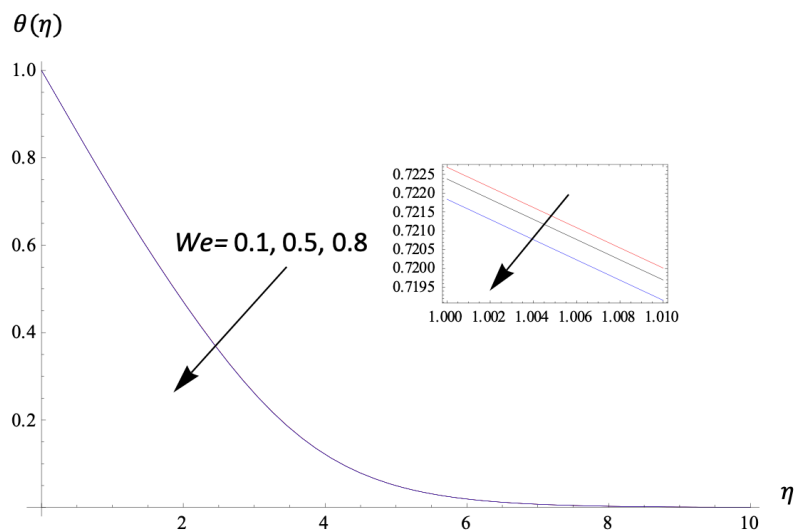


Fig. 10. $\theta(\eta)$ against η for various magnitudes of We with $n = 1.2$, $Pr = 0.7$, $\lambda = 0.1$, $Rd = 1$, and $\varepsilon = Q = 0.2$

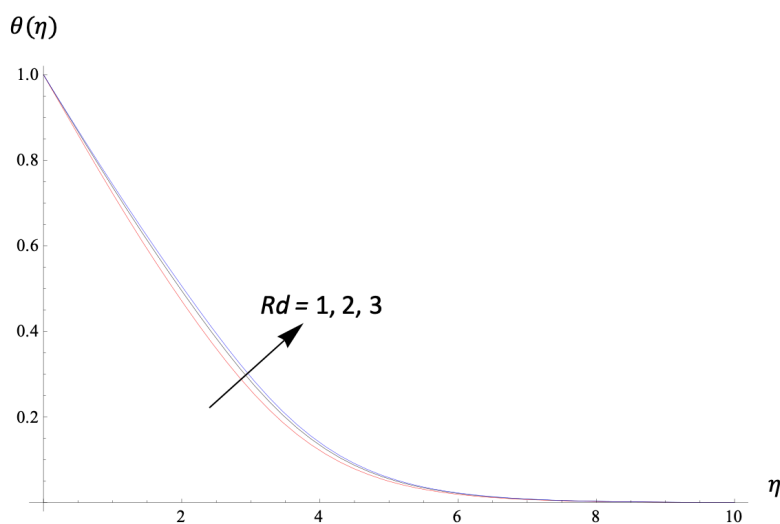


Fig. 11. $\theta(\eta)$ against η for different magnitudes of Rd with $n = 1.2$, $\varepsilon = Q = 0.2$, $Pr = 0.7$, and $\lambda = We = 0.1$

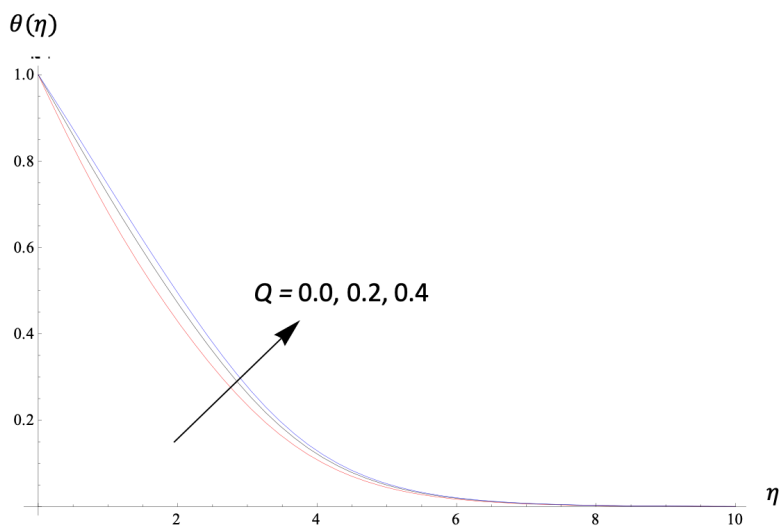


Fig. 12. $\theta(\eta)$ against η for different magnitudes of Q with $\lambda = 0.1$, $Rd = 1$, $We = 0.1$, $Pr = 0.7$, $n = 1.2$, and $\varepsilon = 0.2$.

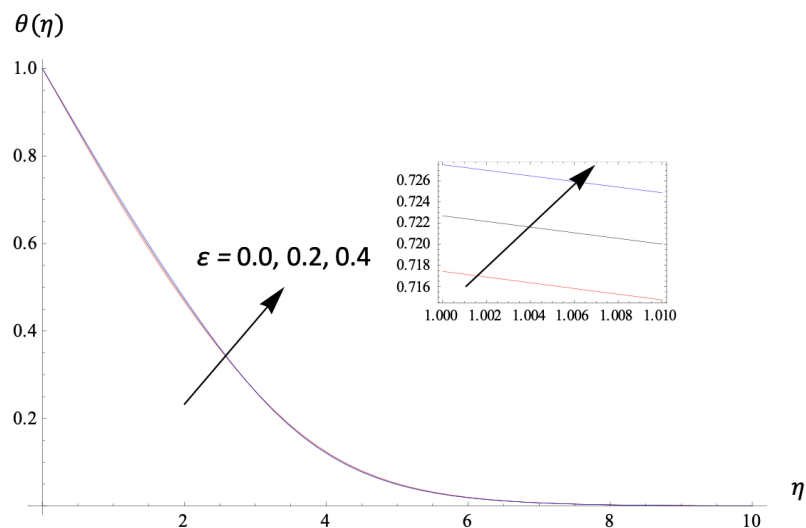


Fig. 13. $\theta(\eta)$ against η for different magnitudes of ϵ with $n = 1.2$, $\epsilon = 0.2$, $Pr = 0.7$, $Rd = 1$, and $\lambda = We = 0.1$

Table 5

The results of the $C_f\sqrt{Re_x}$ for a range of values of We , n , and λ

We	n	λ	C_f/Re
0.1	0.5	0.1	-1.03890
0.5	-	-	-1.01732
0.8	-	-	-0.956351
0.1	1.2	0.1	-1.04012
0.5	-	-	-1.04782
0.8	-	-	-1.05928
0.1	1.4	0.1	-1.04045
-	1.6	-	-1.04078
0.1	1.2	0.5	-1.19653
-	-	1.0	-1.38680

Table 6

The results of the $Nu/\sqrt{Re_x}$ for a range of values of Rd , Pr , ϵ , Q , We , n , and λ

Rd	Pr	ϵ	Q	λ	We	n	Nu/Re
1	0.7	0.2	0.2	0.1	0.1	1.2	-0.278256
2	-	-	-	-	-	-	-0.266297
3	-	-	-	-	-	-	-0.261270
1	1	0.2	0.2	0.1	0.1	1.2	-0.288260
-	2	-	-	-	-	-	-0.338026
1	0.7	0.0	0.2	0.1	0.1	1.2	-0.285406
-	-	0.4	-	-	-	-	-0.272009
1	0.7	0.2	0.0	0.1	0.1	1.2	-0.346583
-	-	-	0.4	-	-	-	-0.241521
1	0.7	0.2	0.2	0.5	0.1	1.2	-0.387327
-	-	-	-	1.0	-	-	-0.506564
1	0.7	0.2	0.2	0.1	0.5	1.2	-0.278624
-	-	-	-	-	0.8	-	-0.279249
1	0.1	0.2	0.2	0.1	0.1	1.4	-0.278271
-	-	-	-	-	-	1.6	-0.278287
-	-	-	-	-	0.1	0.5	-0.278201
-	-	-	-	-	0.5	-	-0.277169
-	-	-	-	-	0.8	-	-0.274279

4. Conclusions

The thermal and Carreau fluid characteristic passing a horizontal stretching cylinder have been concerned, and the influence of thermal radiation and heat source are included. Furthermore, to be more realistic, the thermal conductivity of the Carreau fluid is taken to be dependent on the temperature of the fluid. The similarity conversion technique is utilized to convert the momentum and energy equations into nonlinear ordinary differential equations. Then, the homotopy analysis scheme approximates the analytical solutions of the similarity-transformed governing equations. The method is verified by comparing the current results with the existing solutions for a limiting case in the literature. The method is found appropriate for solving the proposed problem. The effects of the Weissenberg number, heat generation parameter, radiative number, curvature number, and temperature-dependent thermal conductivity on the fluid movement and thermal distribution are discussed. From this investigation, we can conclude:

- The HAM is appropriate to be used to solve the developed highly non-linear ordinary governing equations.
- Q , λ , ε , and Rd accelerate the thermal distribution. In contrast, the n and Pr reduce the temperature.
- A conflict behavior is identified on the temperature profiles due to the Weissenberg number. The temperature shows an increasing function at $n = 0.5$ when We is increased but an opposite tendency is detected when $n = 1.2$.
- For the velocity profiles, the magnitude is enhanced when We is amplified for $n = 1.2$. Contradicting, the momentum thickness is reduced when $n = 0.5$ and We is enhanced.
- The velocity profile is improved by the λ and n .

Acknowledgment

First of all, thanks to all the reviewers and researchers, too many to name, who have given comments and suggestions in completing the current study. This research is financially supported by vote numbers FRGS/1/2019/STG06/UTM/02/22, and UTMSHine grant 09G88. The support of the RMC-UTM and the Ministry of Higher Education Malaysia is appreciated.

References

- [1] Carreau, Pierre J. "Rheological equations from molecular network theories." *Transactions of the Society of Rheology* 16, no. 1 (1972): 99-127. <https://doi.org/10.1122/1.549276>
- [2] El Misery, A. E. M., and M. F. Abd El Kareem. "Separation in the flow through peristaltic motion of a Carreau fluid in uniform tube." *Physica A: Statistical Mechanics and Its Applications* 343 (2004): 1-14. <https://doi.org/10.1016/j.physa.2004.05.072>
- [3] Akbar, Noreen Sher, and S. Nadeem. "Combined effects of heat and chemical reactions on the peristaltic flow of Carreau fluid model in a diverging tube." *International journal for numerical methods in fluids* 67, no. 12 (2011): 1818-1832. <https://doi.org/10.1002/flid.2447>
- [4] Akbar, N. S., S. Nadeem, Rizwan Ul Haq, and Shiwei Ye. "MHD stagnation point flow of Carreau fluid toward a permeable shrinking sheet: Dual solutions." *Ain Shams Engineering Journal* 5, no. 4 (2014): 1233-1239. <https://doi.org/10.1016/j.asej.2014.05.006>
- [5] Hayat, Tasawar, Sadia Asad, Meraj Mustafa, and Ahmed Alsaedi. "Boundary layer flow of Carreau fluid over a convectively heated stretching sheet." *Applied Mathematics and Computation* 246 (2014): 12-22. <https://doi.org/10.1016/j.amc.2014.07.083>
- [6] Khan, Masood. "Boundary layer flow and heat transfer to Carreau fluid over a nonlinear stretching sheet." *AIP Advances* 5, no. 10 (2015): 107203. <https://doi.org/10.1063/1.4932627>
- [7] Hayat, T., M. Waqas, S. A. Shehzad, and A. Alsaedi. "Stretched flow of Carreau nanofluid with convective boundary condition." *Pramana* 86, no. 1 (2016): 3-17. <https://doi.org/10.1007/s12043-015-1137-y>

- [8] Khan, M., M. Irfan, W. A. Khan, and A. S. Alshomrani. "A new modeling for 3D Carreau fluid flow considering nonlinear thermal radiation." *Results in physics* 7 (2017): 2692-2704. <https://doi.org/10.1016/j.rinp.2017.07.024>
- [9] Wang, Ch Y. "Fluid flow due to a stretching cylinder." *The Physics of fluids* 31, no. 3 (1988): 466-468. <https://doi.org/10.1063/1.866827>
- [10] Salahuddin, T. "Carreau fluid model towards a stretching cylinder: Using Keller box and shooting method." *Ain Shams Engineering Journal* 11, no. 2 (2020): 495-500. <https://doi.org/10.1016/j.asej.2017.03.016>
- [11] Khan, Masood, and Ali Saleh Alshomrani. "Characteristics of melting heat transfer during flow of Carreau fluid induced by a stretching cylinder." *The European Physical Journal E* 40, no. 1 (2017): 1-9. <https://doi.org/10.1140/epje/i2017-11495-6>
- [12] Salahuddin, T., Arif Hussain, M. Y. Malik, M. Awais, and Mair Khan. "Carreau nanofluid impinging over a stretching cylinder with generalized slip effects: using finite difference scheme." *Results in physics* 7 (2017): 3090-3099. <https://doi.org/10.1016/j.rinp.2017.07.036>
- [13] Hayat, T., Ikram Ullah, B. Ahmad, and A. Alsaedi. "Radiative flow of Carreau liquid in presence of Newtonian heating and chemical reaction." *Results in Physics* 7 (2017): 715-722. <https://doi.org/10.1016/j.rinp.2017.01.019>
- [14] Khan, Imad, M. Y. Malik, Arif Hussain, and Mair Khan. "Magnetohydrodynamics Carreau nanofluid flow over an inclined convective heated stretching cylinder with Joule heating." *Results in physics* 7 (2017): 4001-4012. <https://doi.org/10.1016/j.rinp.2017.10.015>
- [15] Gangadhar, K., K. V. Ramana, Oluwole Daniel Makinde, and B. Rushi Kumar. "MHD flow of a Carreau fluid past a stretching cylinder with Cattaneo-Christov heat flux using spectral relaxation method." In *Defect and Diffusion Forum*, vol. 387, pp. 91-105. Trans Tech Publications Ltd, 2018. <https://doi.org/10.4028/www.scientific.net/DDF.387.91>
- [16] Gopal, D., and N. Kishan. "Unsteady flow of a Carreau fluid over a shrinking cylinder in the occurrence of various parameter effects." In *AIP Conference proceedings*, vol. 2104, no. 1, p. 020004. AIP Publishing LLC, 2019. <https://doi.org/10.1063/1.5100372>
- [17] Song, Ying-Qing, Hassan Waqas, Kamel Al-Khaled, Umar Farooq, Soumaya Gouadria, Muhammad Imran, Sami Ullah Khan, M. Ijaz Khan, Sumaira Qayyum, and Qiu-Hong Shi. "Aspects of thermal diffusivity and melting phenomenon in Carreau nanofluid flow confined by nonlinear stretching cylinder with convective Marangoni boundary constraints." *Mathematics and Computers in Simulation* 195 (2022): 138-150. <https://doi.org/10.1016/j.matcom.2022.01.001>
- [18] Akram, Mohammad, Wasim Jamshed, B. Shankar Goud, Amjad Ali Pasha, Tanveer Sajid, M. M. Rahman, Misbah Arshad, and Wajaree Weera. "Irregular heat source impact on carreau nanofluid flowing via exponential expanding cylinder: A thermal case study." *Case Studies in Thermal Engineering* (2022): 102171. <https://doi.org/10.1016/j.csite.2022.102171>
- [19] Kardri, Mahani Ahmad, Norfifah Bachok, Norihan Md Arifin, Fadzilah Md Ali, and Yong Faezah Rahim. "Magnetohydrodynamic Flow Past a Nonlinear Stretching or Shrinking Cylinder in Nanofluid with Viscous Dissipation and Heat Generation Effect." *Journal of Advanced Research in Fluid Mechanics and Thermal Sciences* 90, no. 1 (2022): 102-114. <https://doi.org/10.37934/arfmts.90.1.102114>
- [20] Chiam, TC0914. "Heat transfer in a fluid with variable thermal conductivity over a linearly stretching sheet." *Acta mechanica* 129, no. 1 (1998): 63-72. <https://doi.org/10.1007/BF01379650>
- [21] Arunachalam, M., and N. R. Rajappa. "Thermal boundary layer in liquid metals with variable thermal conductivity." *Flow, Turbulence and Combustion* 34, no. 2 (1978): 179-187. <https://doi.org/10.1007/BF00418866>
- [22] Kays, W.M., *Convective heat and mass transfer*. 2011: Tata McGraw-Hill Education.
- [23] Arunachalam, M., and N. R. Rajappa. "Forced convection in liquid metals with variable thermal conductivity and capacity." *Acta Mechanica* 31, no. 1 (1978): 25-31. <https://doi.org/10.1007/BF01261185>
- [24] Khan, Ambreen A., S. Naeem, R. Ellahi, Sadiq M. Sait, and K. Vafai. "Dufour and Soret effects on Darcy-Forchheimer flow of second-grade fluid with the variable magnetic field and thermal conductivity." *International Journal of Numerical Methods for Heat & Fluid Flow* (2020). <https://doi.org/10.1108/HFF-11-2019-0837>
- [25] Swain, Kharabela, Basavarajappa Mahanthesh, and Fateh Mebarek-Oudina. "Heat transport and stagnation-point flow of magnetized nanoliquid with variable thermal conductivity, Brownian moment, and thermophoresis aspects." *Heat Transfer* 50, no. 1 (2021): 754-767. <https://doi.org/10.1002/htj.21902>
- [26] Khan, Sami Ullah, and Sabir Ali Shehzad. "Electrical MHD Carreau nanofluid over porous oscillatory stretching surface with variable thermal conductivity: applications of thermal extrusion system." *Physica A: Statistical Mechanics and its Applications* 550 (2020): 124132. <https://doi.org/10.1016/j.physa.2020.124132>
- [27] Abbas, Tariq, Sajid Rehman, Rehan Ali Shah, Muhammad Idrees, and Mubashir Qayyum. "Analysis of MHD Carreau fluid flow over a stretching permeable sheet with variable viscosity and thermal conductivity." *Physica A: Statistical Mechanics and its Applications* 551 (2020): 124225. <https://doi.org/10.1016/j.physa.2020.124225>

- [28] Yin, Junfeng, Xianqin Zhang, M. Israr Ur Rehman, and Aamir Hamid. "Thermal radiation aspect of bioconvection flow of magnetized Sisko nanofluid along a stretching cylinder with swimming microorganisms." *Case Studies in Thermal Engineering* 30 (2022): 101771. <https://doi.org/10.1016/j.csite.2022.101771>
- [29] Nabwey, Hossam A., Sumayyah I. Alshber, Ahmed M. Rashad, and Abd El Nasser Mahdy. "Influence of bioconvection and chemical reaction on magneto—Carreau nanofluid flow through an inclined cylinder." *Mathematics* 10, no. 3 (2022): 504. <https://doi.org/10.3390/math10030504>
- [30] Hayat, T., S. Asad, and A. Alsaedi. "Flow of variable thermal conductivity fluid due to inclined stretching cylinder with viscous dissipation and thermal radiation." *Applied Mathematics and Mechanics* 35, no. 6 (2014): 717-728. <https://doi.org/10.1007/s10483-014-1824-6>
- [31] Jain, Shalini, and Amit Parmar. "Radiation effect on MHD williamson fluid flow over stretching cylinder through porous medium with heat source." In *Applications of Fluid Dynamics*, pp. 61-78. Springer, Singapore, 2018. https://doi.org/10.1007/978-981-10-5329-0_5
- [32] Salahuddin, T., M. Y Malik, Arif Hussain, and S. Bilal. "Combined effects of variable thermal conductivity and MHD flow on pseudoplastic fluid over a stretching cylinder by using Keller box method." *Information Sciences Letters* 5, no. 1 (2016): 2. <https://doi.org/10.18576/isl/050102>
- [33] Malik, M. Y., M. Bibi, Farzana Khan, and T. Salahuddin. "Numerical solution of Williamson fluid flow past a stretching cylinder and heat transfer with variable thermal conductivity and heat generation/absorption." *AIP Advances* 6, no. 3 (2016): 035101. <https://doi.org/10.1063/1.4943398>
- [34] Rangi, Rekha R., and Naseem Ahmad. "Boundary layer flow past a stretching cylinder and heat transfer with variable thermal conductivity." (2012). <https://doi.org/10.4236/am.2012.33032>
- [35] Ewis, Karem Mahmoud. "Effects of Variable Thermal Conductivity and Grashof Number on Non-Darcian Natural Convection Flow of Viscoelastic Fluids with Non Linear Radiation and Dissipations." *Journal of Advanced Research in Applied Sciences and Engineering Technology* 22, no. 1 (2021): 69-80. <https://doi.org/10.37934/araset.22.1.6980>
- [36] Liao, Shijun. *Beyond perturbation: introduction to the homotopy analysis method*. Chapman and Hall/CRC, 2003.
- [37] Liao, Shijun. "Notes on the homotopy analysis method: some definitions and theorems." *Communications in Nonlinear Science and Numerical Simulation* 14, no. 4 (2009): 983-997. <https://doi.org/10.1016/j.cnsns.2008.04.013>
- [38] Liao, Shijun. *Homotopy analysis method in nonlinear differential equations*. Beijing: Higher education press, 2012. <https://doi.org/10.1007/978-3-642-25132-0>
- [39] Patel, Vijay K., and Jigisha U. Pandya. "The Consequences of Thermal Radiation and Chemical Reactions on Magneto-hydrodynamics in Two Dimensions over a Stretching Sheet with Jeffrey Fluid." *Journal of Advanced Research in Fluid Mechanics and Thermal Sciences* 95, no. 1 (2022): 121-144. <https://doi.org/10.37934/arfmts.95.1.121144>
- [40] Thirupathi, Gurralla, Kamatam Govardhan, and Ganji Narender. "Radiative Magnetohydrodynamics Casson Nanofluid Flow and Heat and Mass Transfer past on Nonlinear Stretching Surface." *Journal of Advanced Research in Numerical Heat Transfer* 6, no. 1 (2021): 1-21. <https://doi.org/10.3762/bxiv.2021.65.v1>
- [41] Hayat, T., M. S. Anwar, M. Farooq, and A. Alsaedi. "MHD stagnation point flow of second grade fluid over a stretching cylinder with heat and mass transfer." *International Journal of Nonlinear Sciences and Numerical Simulation* 15, no. 6 (2014): 365-376. <https://doi.org/10.1515/ijnsns-2013-0104>
- [42] Elbashbeshy, E. M. A., T. G. Emam, M. S. El-Azab, and K. M. Abdelgaber. "Effect of magnetic field on flow and heat transfer over a stretching horizontal cylinder in the presence of a heat source/sink with suction/injection." *J. Appl. Mech. Eng* 1, no. 1 (2012): 1-5. <https://doi.org/10.4172/2168-9873.1000106>
- [43] Poply, Vikas, Phool Singh, and K. K. Chaudhary. "Analysis of laminar boundary layer flow along a stretching cylinder in the presence of thermal radiation." *WSEAS Trans Fluid Mech* 8, no. 4 (2013): 159-164.